European Heart Journal (2006) **27**, 2560–2566
doi:10.1093/eurheartj/ehl288

Analysis of myocardial deformation based on ultrasonic pixel tracking to determine transmurality in chronic myocardial infarction

Michael Becker[1†], Rainer Hoffmann[1*†], Harald P. Kühl[1], Helena Grawe[1], Markus Katoh[2], Rafael Kramann[1], Arno Bücker[2], Peter Hanrath[1], and Nicole Heussen[3]

[1] *Medical Clinic I, University Hospital RWTH Aachen, Pauwelsstraße 30, 52057 Aachen, Germany;* [2] *Department of Radiology, University Hospital RWTH Aachen, Pauwelsstraße 30, 52057 Aachen, Germany; and* [3] *Department of Medical Statistics, University Hospital RWTH Aachen, Pauwelsstraße 30, 52057 Aachen, Germany*

Received 2 January 2006; revised 10 September 2006; accepted 14 September 2006; online publish-ahead-of-print 11 October 2006

KEYWORDS
Echocardiography;
Magnetic resonance imaging;
Myocardial infarction;
Viability

Aims Pixel tracking-derived myocardial deformation imaging is a new echocardiographic modality which allows quantitative analysis of segmental myocardial function on the basis of tracking of natural acoustic markers in 2D echocardiography. This study evaluated whether myocardial deformation parameters calculated from 2D echocardiography allow assessment of transmurality of myocardial infarction as defined by contrast-enhanced cardiac magnetic resonance imaging (ceMRI).
Methods In 47 patients with ischaemic left ventricular dysfunction, transmurality of myocardial infarction was assessed using pixel-tracking-derived myocardial deformation imaging and ceMRI. For each left ventricular segment in a 16-segment model, peak systolic radial strain, circumferential strain, radial strain rate, and circumferential strain rate were calculated from parasternal 2D echocardiographic views using an automatic frame-by-frame tracking system of natural acoustic echocardiographic markers (EchoPAC, GE Ultrasound). Myocardial deformation parameters were related to the segmental extent of hyperenhancement by ceMRI. The relative amount of contrast-enhanced myocardial tissue per segment was used to define no infarction (0% hyperenhancement), non-transmural infarction (1–50% hyperenhancement), or transmural infarction (51–100% hyperenhancement).
Results Analysis of myocardial deformation parameters was possible in 659 segments (88%). Systolic strain and strain rate parameters decreased with increasing relative hyperenhancement defined by ceMRI. Radial strain was 27.7 ± 8.0, 20.5 ± 9.7, and 11.6 ± 8.5% for segments with no infarction ($n = 422$), non-transmural infarction ($n = 106$), and transmural infarction ($n = 131$), respectively ($P < 0.0001$). Radial strain allowed distinction of non-transmural infarction from transmural infarction with a sensitivity of 70.0% and a specificity of 71.2% (cut-off value for radial strain 16.5%).
Conclusion Frame-to-frame tracking of acoustic markers in 2D echocardiographic images for the analysis of myocardial deformation allows discrimination between different transmurality states of myocardial infarction.

Introduction

The identification of myocardial viability in patients with depressed left ventricular (LV) function has important therapeutic and prognostic implications.[1] Different imaging modalities analysing the functional, cellular, or metabolic integrity have been used for the assessment of myocardial viability in patients with chronic myocardial infarction.[2–4] Contrast-enhanced magnetic resonance imaging (ceMRI) has evolved into the non-invasive reference technique for the analysis of myocardial viability in chronic ischaemic heart disease, as it allows direct visualization of the transmural extent of necrotic non-viable tissue.[5–7]

Doppler ultrasound-based myocardial strain imaging allows accurate quantification of regional myocardial deformation.[8,9] In experimental studies, Doppler ultrasound-based strain-imaging modalities have proved to permit differentiation of transmural myocardial infarction from non-transmural myocardial infarction.[10,11] However, Doppler-based strain imaging is affected by a significant angle dependency and possible noise artefacts.[12] Thus, although a very valuable method in experimental studies, the difficulties of Doppler-based strain analysis have limited its use in clinical practice.

Recently, a 2D echocardiographic imaging technique has been described, which allows quantification of myocardial deformation on the basis of tracking of acoustic markers from frame-to-frame.[13,14] Because of the conceptual difference of this method from Doppler-based techniques, it is

* Corresponding author. Tel: +49 241 8088468; fax: +49 241 8082303.
E-mail address: rhoffmann@ukaachen.de
† The first two authors have contributed equally.

angle-independent. It may allow an accurate assessment of regional myocardial deformation and thereby a reliable analysis of the transmural extent of necrosis even under challenging clinical circumstances.

In this study, we sought to evaluate whether myocardial deformation parameters derived from the tracking of acoustic markers within 2D echocardiographic images allow accurate assessment of the transmural extent of myocardial necrosis in patients with LV dysfunction due to chronic ischaemic heart disease. The transmural extent of necrosis was defined by ceMRI.

Methods

Study population

Between August 2004 and July 2005, 109 patients with impaired LV function underwent MRI for the definition of myocardial viability. Fifty-nine patients with non-ischaemic cardiomyopathy or acute coronary syndromes were excluded from the study to avoid possible stunning or acute ischaemia. Within the 50 patients with chronic ischaemic heart disease, three patients refused participation in the current study and 47 patients gave written informed consent. Coronary angiography, cineventriculography, and 2D echocardiography with myocardial deformation imaging were performed in all these patients. This study was approved by the local Ethical Committee.

Echocardiography

Within a few hours after MRI, echocardiograms were performed with a Vivid Seven System (GE Vingmed, Horton, Norway) equipped with a 2.5 MHz transducer. LV parasternal short-axis views at basal, midventricular, and apical levels were acquired and processed. The frame rate for these studies was between 56 and 92 frame(s) using tissue harmonic imaging. LV ejection fraction was determined by manual tracing of end-systolic and end-diastolic endocardial borders, using apical four-chamber and two-chamber views, employing biplane Simpson's method. The LV was divided according to the 16-segment model of the American Society of Echocardiography.[15]

Pixel-tracking-based strain and strain rate analysis

The three acquired parasternal short-axis views at basal, midventricular, and apical level were analysed considering the 16-segment model (six segments for the basal and midventricular short-axis view and four segments for the apical short-axis view). Analysis was performed offline with the aid of a dedicated software package (EchoPAC BT 05.2, GE Vingmed, Horton, Norway). This system allows analysis of peak systolic radial strain and circumferential strain and strain rate (SR) on the basis of the detection of natural acoustic markers. These markers are acoustic speckles that are equally distributed within the myocardium and can be identified as well as followed frame-to-frame during several consecutive images.[13,14] The natural acoustic markers are expected to change their position from frame-to-frame in accordance with the surrounding tissue motion.[14] The system calculates mean strain and SR values for whole predefined LV segments, including all myocardial layers from the endocardium to epicardium.

Regarding the tracking quality, the system automatically generates a scale ranging from 1.0 for optimal to 3.0 for unacceptable for each analysed segment, as described earlier.[14] We systematically dismissed segments with suboptimal tracking quality (grading >2.0 by the system) from the analysis. For the remaining segments, visual control of tracking quality was performed to ensure adequate automatic tracking. End-systole was determined in the apical long-axis view as aortic valve closure. The time difference from the QRS complex was transferred to the other views. A medium degree of spatial and temporal smoothing was selected in the analysis algorithm of deformation parameters.

For each LV segment with adequate tracking quality, peak systolic radial strain, peak systolic circumferential strain, peak systolic radial SR, and peak systolic circumferential SR were automatically calculated. Circumferential strain and SR as parameters of circumferential deformation relate to deformation along the curvature of the left ventricle in the parasternal short axis. Radial strain and SR relate to deformation (thickening or thinning) from the endocardium to the epicardium. SR is equivalent to the spatial gradient of pixel movements. Thus, it resembles the equation for SR reported for Doppler imaging techniques.

To determine the relation between radial strain and systolic wall thickening, segmental systolic wall thickening was determined from end-systolic and end-diastolic images and related to radial strain in 145 segments with sufficient image quality from 10 patients. There was a good correlation between radial strain and systolic wall thickening ($r = 0.93$, $P < 0.001$). To define intraobserver and interobserver agreement in acquisition of myocardial deformation parameters, in 10 subjects, strain and SR analysis was repeated 4 weeks apart by the same observer on the same 2D echocardiographic loop and the same cardiac cycle and performed in addition by a second independent observer. As an aggregate measure for agreement, a coefficient according to Lin,[16] with maximum range between -1 and $+1$, was calculated. It represents for continuous data an analogue of the weighted κ coefficient determined for ordinal data. For intraobserver agreement, the Lin coefficient was 0.95 [95% confidence interval (CI) 0.90–1.00] for circumferential strain, 0.92 (95% CI 0.88–0.96) for circumferential SR, 0.99 (95% CI 0.98–0.99) for radial strain, and 0.96 (95% CI 0.93–0.98) for radial SR. For interobserver agreement, the Lin coefficient was 0.93 (95% CI 0.89–0.97) for circumferential strain, 0.73 (95% CI 0.62–0.84) for circumferential SR, 0.96 (95% CI 0.94–0.98) for radial strain, and 0.84 (95% CI 0.77–0.91) for radial SR.

Contrast-enhanced cardiac magnetic resonance imaging

All patients underwent ceMRI within a few hours of the echocardiographic study on a 1.5 T whole-body MR scanner (Intera, Best, Philips, the Netherlands) using a five-element phased-array cardiac coil, with the patient placed supine. Fifteen minutes after intravenous injection of 0.2 mmol/kg body-weight Gd-DTPA (Magnevist, Schering, Berlin, Germany), 8 mm short-axis slices were acquired with a prospectively electocardiogram-gated gradient echo sequence with inversion prepulse. Imaging parameters were as follows: repetition time (TR) two heartbeats, echo time (TE) 5.0 ms, flip angle 25°, field of view 380×380 mm^2, 256×256 matrix, and in-plane resolution 1.5 mm^2. The inversion time of the pre-pulse varied according to subjective visual judgement from 275 to 300 ms in order to achieve optimal signal suppression of normal myocardium and, consequently, optimal image contrast between infarcted and viable myocardium. Images were subsequently transferred to a workstation equipped with a dedicated cardiac software package (MassSoftware, Medis, Leiden, the Netherlands) for further analysis. Magnetic resonance imaging data were assessed by an experienced reader blinded to clinical data and results of the other imaging technique. LV mass and infarct mass were determined by manual tracing of endocardial and epicardial border as well as tracing of hyperenhancement borders, using systolic short-axis views, employing Simpson's method.

The assignment to a hyperenhancement category reflects the extent of hyperenhancement within each segment by visual assessment considering a five-group scale proposed by Kim *et al.*[17]: 0% hyperenhancement (group 1), 1–25% hyperenhancement (group 2), 26–50% hyperenhancement (group 3), 51–75% hyperenhancement

(group 4), and 76–100% hyperenhancement (group 5); 0% hyperenhancement was considered to reflect non-infarction; groups 2 and 3 (hyperenhancement 1–50%) were combined and were considered to reflect non-transmural infarction, whereas groups 4 and 5 (hyperenhancement 51–100%) were combined and considered to reflect transmural infarction as proposed before.[18] Intraobserver and interobserver agreement in the visual analysis of ceMRI was tested in 10 ceMRI studies (160 segments). The weighted κ coefficient for ordinal data was used considering all five hyperenhancement categories. Cohen's κ coefficient for nominal data was calculated considering only assessment as non-transmural or transmural.[19] The intraobserver agreement was found to be weighted $\kappa = 0.78$ (95% CI 0.56–0.99) considering all five hyperenhancement groups and $\kappa = 0.85$ (95%CI 0.77–0.93) considering only assessment as non-transmural or transmural. The interobserver agreement was found to be weighted $\kappa = 0.75$ (95% CI 0.54–0.96) considering all five hyperenhancement groups and $\kappa = 0.83$ (95%CI 0.75–0.91) considering only assessment as non-transmural or transmural. In addition, the maximal thickness of myocardial tissue without late hyperenhancement was determined for each LV segment. This was considered to be a parameter of the remaining viable myocardium.

Coronary angiography and cineventriculography

The severity of coronary stenosis was determined quantitatively using a commercially available software (QuantCor, CASS II, Siemens, Erlangen, Germany). Significant coronary artery stenosis was considered present when >50% reduction of vessel diameter was observed in at least one major coronary artery. Monoplane planimetry of cineventriculograms was performed to determine LV ejection fraction.

Statistics

Data are expressed as means $\pm$ standard deviation. A reasonable assumption is that the observations in a patient are correlated; therefore, a repeated measures analysis of variance (rmANOVA) was applied to compare mean deformation values among patients with hyperenhancement 0% (normal), 1–50% (non-transmural), and 51%–100% (transmural infarction). The fitted covariance structure of compound symmetry implies that the covariance between repeated measures is due to the patient contribution. Only fixed effects are included in the model. For each parameter, the effect of late enhancement group, segment, and late enhancement group by segment interaction was assessed. In the case of significant group effect, *post hoc* comparisons between groups of normal and non-transmural and non-transmural and transmural segments were added.

For estimating sensitivity and specificity, a generalized estimating equation (GEE) approach was used with a Bernoulli variance function, a logistic link, and a working correlation matrix with exchangeable correlation assumption. This GEE model is identical to a logistic regression model logit $P = \beta_0 + \beta_1 X_1$ (with (1) P the probability that the observed value is less or equal than the actual cut off value, X_1 the late enhancement 0 respectively 1 or 2 for discrimination between no infarction vs. non-transmural infarction or (2) P the probability that the observed value is greater than the actual cut off value, X_1 the late enhancement 1 or 2 respectively 3 or 4 for discrimination between non-transmural vs. transmural infarction, β_0 the intercept, β_1 the regression coefficient of late enhancement) in which correlation between observations in a patient is taken into account. Therefore, sensitivity may be calculated as $[\exp(\beta_0 + \beta_1)]/[1 + \exp(\beta_0 + \beta_1)]$ and specificity as $1/[1 + \exp(\beta_0)]$. To increase the accuracy for the detection of segments with non-transmural infarction vs. segments with transmural infarction or non-infarcted segments, we decided to keep the sensitivity fixed. The cut-off values for circumferential strain, circumferential SR, radial strain, and radial SR were therefore set in order to obtain a minimum sensitivity of 70% and maximize specificity over the set of eligible cut-off values such that sensitivity does not fall below this minimum. Because of the fact that cut-off values with repeated estimation of regression coefficients and calculation of sensitivities and specificities were based on the same data, obtained results may be too optimistic. To evaluate the degree of overoptimism, we calculated sensitivity and specificity from bootstrap samples and provided mean and, additionally, confidence limits on the basis of bootstrap percentiles.[20] To give a description of the possible dispersion of cut-off values, we derived for each bootstrap sample the value for which a minimum sensitivity of 70% attains maximum specificity and calculated mean values as well as confidence limits. For all calculations, we included 1000 bootstrap samples of the original data in which sample size equals the sample size of the original data and estimated for each sample regression coefficients to calculate sensitivity and specificity in the earlier-described model.

To assess the influence of wall thickness without hyperenhancement on circumferential strain, circumferential SR, radial strain, and radial SR, a repeated measures analysis of covariance (rmANCOVA) with compound symmetry correlation assumption was conducted. For each parameter, the fixed effect of wall thickness as covariate, segment, and wall thickness by segment interaction was assessed. Applied tests were two-sided, and resulting *P*-values less than an alpha level of 0.05 were considered to indicate statistical significance. In the case of *post hoc* comparisons, Bonferroni correction was applied. All statistical analyses were performed using SAS Release 8.02 (SAS Institute Inc., Cary, NC, USA).

Table 1 Clinical characteristics

	Patients ($n = 47$)
Age (years)	57.5 $\pm$ 8.3
Gender (males)	36
Heart rate (b.p.m.)	73.3 $\pm$ 10.2
History of myocardial infarction, *n* (%)	37 (86)
Ejection fraction (%)	41 $\pm$ 11
Coronary artery disease	
One-vessel disease, *n* (%)	12 (26)
Two-vessel disease, *n* (%)	17 (36)
Three-vessel disease, *n* (%)	18 (38)

Results

Clinical baseline characteristics of the patients are given in *Table 1*. Significant coronary artery stenosis (>50% diameter stenosis) was documented in all patients. The image quality allowed analysis of strain and SR parameters by tracking of acoustic markers in the 2D echocardiographic images in 659 segments (88%).

Cardiac magnetic resonance imaging

Total LV mass defined by MRI was 146 $\pm$ 35 g and total infarct size 27 $\pm$ 20 g (18.5 $\pm$ 13.5%). Among the 659 segments with adequate tracking of acoustic markers, segmental analysis of ceMRI indicated 0% hyperenhancement in 422 segments, 1–25% hyperenhancement in 56 segments, 26–50% hyperenhancement in 50 segments, 51–75% hyperenhancement in 80 segments, and 76–100% hyperenhancement in 51 segments. There were 106 segments with late hyperenhancement 1–50% (non-transmural infarcts) and 131 segments with late hyperenhancement 51–100% (transmural infarcts).

Table 2 Myocardial deformation parameters related to relative degree of myocardial hyperenhancement by ceMRI

Segmental hyperenhancement	Circumferential strain (%)	Radial strain (%)	Circumferential SR (s^{-1})	Radial SR (s^{-1})
0%, non-infarcted ($n = 422$)	-18.6 ± 5.6	27.7 ± 8.0	-1.42 ± 0.34	1.43 ± 0.55
1–50%, non-transmural infarction ($n = 106$)	-12.8 ± 6.7	20.5 ± 9.7	-1.07 ± 0.48	1.12 ± 0.37
51–100%, transmural infarction ($n = 131$)	-8.1 ± 5.3	11.6 ± 8.5	-0.81 ± 0.44	0.79 ± 0.45
rmANOVA (all groups of hyperenhancement)	<0.0001	<0.0001	<0.0001	<0.0001
Post hoc test [normal (group 1) vs. non-transmural late enhance-ment (groups 2 and 3)]	<0.0002	<0.0002	<0.0002	<0.0002
Post hoc test [non-transmural (groups 2 and 3) vs. transmural late enhancement (groups 4 and 5)]	0.0016	0.0458	<0.0002	0.0020

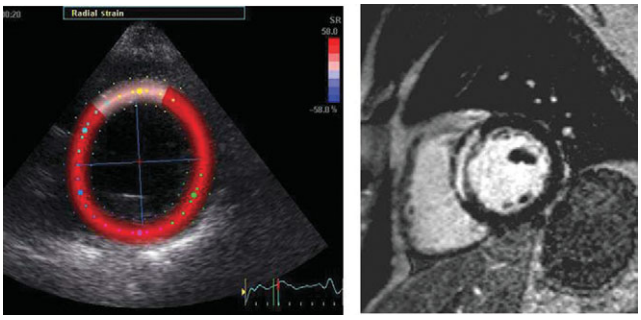

Figure 1 Colour-coded short-axis radial strain image at end-systole (left panel) and ceMRI image (right panel) of a patient with akinesia and transmural infarction of the septal wall by ceMRI (>50% hyperenhancement). There is red colourization in the normal contracting segments with no hyperenhancement, whereas there is only purple colourization in the segment showing no wall thickening and a high amount of hyperenhancement in the ceMRI image.

Strain and SR related to hyperenhancement by ceMRI

The results of peak systolic radial and circumferential strain and SR related to segmental hyperenhancement defined by ceMRI are given in *Table 2*. There were significant differences in all myocardial deformation parameters among non-infarcted segments, segments with non-transmural infarction, and transmural infarction. The greater the transmural degree of hyperenhancement, the lower the myocardial deformation values. In segments with 51–100% hyperenhancement by ceMRI, the radial strain was 44% lower (relative deviation) compared with radial strain of segments with 1–50% late enhancement. Radial strain was 27.7 ± 8.0, 20.5 ± 9.7, and 11.6 ± 8.5% for non-infarcted segments, segments with non-transmural infarction, and transmural infarction, respectively ($P < 0.0001$). *Post hoc* analysis demonstrated also significant differences in myocardial deformation parameters of non-infarcted segments compared with segments with non-transmural infarction and between segments with non-transmural infarction compared with segments with transmural infarction (*Table 2*).

Figures 1 and *2* demonstrate transmural hyperenhancement by ceMRI, with the corresponding radial strain image showing low segmental radial strain, and *Figures 3* and *4* demonstrate non-transmural hyperenhancement by ceMRI, with the corresponding radial strain image showing considerably higher segmental radial strain.

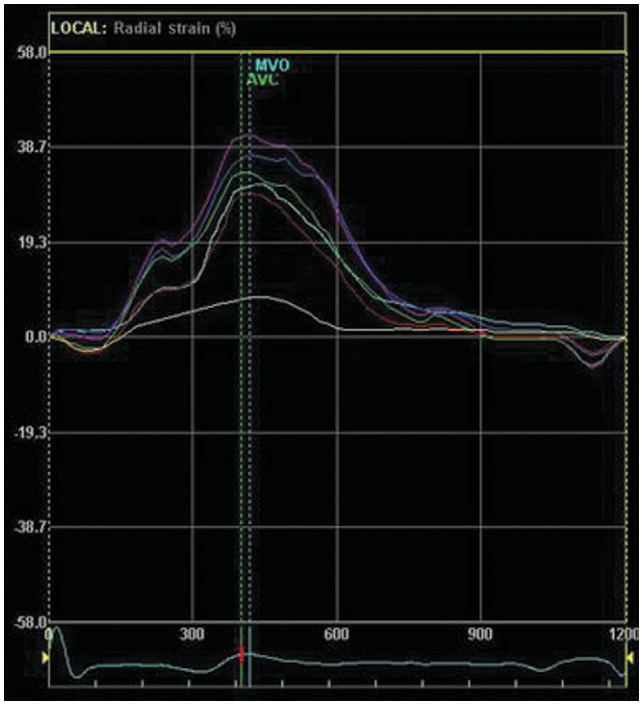

Figure 2 Radial strain tracings for one cardiac cycle obtained from the parasternal short-axis view in the patient with akinesia of the septal wall. There are six tracings for the six evaluated segments within the circumference. The SR tracing of the septal segment demonstrates a low peak systolic radial strain compared with the other segments.

Distinction of non-transmural vs. transmural infarction

Considering the hyperenhancement findings by ceMRI, radial and circumferential strain and SR analysis allowed distinction of segments with non-transmural vs. transmural infarction. A peak systolic radial strain >16.5% had a data-based sensitivity of 70.0% and a specificity of 71.2% to detect non-transmural infarction defined by ceMRI (*Table 3*). For the peak systolic radial SR, a sensitivity of 70.1% and a specificity of 70.6% to detect non-transmural infarction defined by ceMRI were calculated considering a cut-off value of 1.06 s^{-1}. Similar sensitivities and specificities for the detection of non-transmural hyperenhancement were determined for circumferential strain and SR. Data-based and bootstrap-based sensitivities and specificities as well as the corresponding 95% CI for all myocardial deformation parameters are given in *Table 3*.

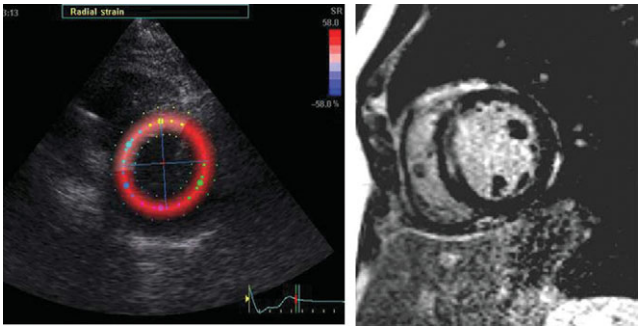

Figure 3 Colour-coded short-axis radial strain images at end-systole (left panel) and ceMRI images (right panel) of a patient with severe hypokinesia and non-transmural infarction of the septal wall by ceMRI (≤50% hyperenhancement). There is red colourization in the normal contracting segments with no hyperenhancement, whereas there is light red colourization in the segment showing less wall thickening and hyperenhancement in the ceMRI images.

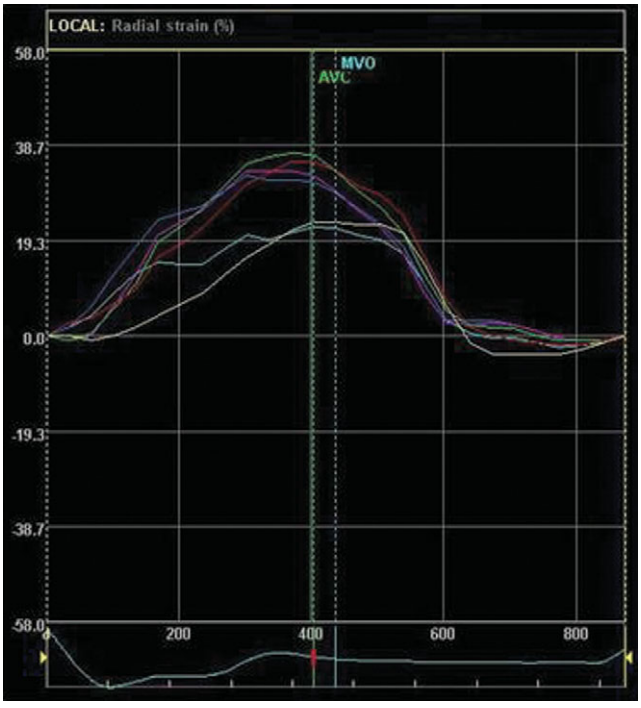

Figure 4 Radial strain tracings for one cardiac cycle obtained from the parasternal short-axis view in the patient with severe hypokinesia of the septal wall. There are six tracings for the six evaluated segments within the circumference. The SR tracing of the septal segment demonstrates a reduced peak systolic radial strain.

Distinction of non-transmural infarction vs. no infarction

Additionally, radial and circumferential strain and SR analysis allowed distinction of segments with non-transmural infarction vs. non-infarcted tissue. A peak systolic radial strain $<27.1\%$ had a sensitivity of 70.1% and a specificity of 57.2% to detect non-transmural infarction defined by ceMRI. A peak radial SR $<1.35\,s^{-1}$, circumferential strain $>-16.5\%$, and circumferential SR $>-1.40\,s^{-1}$ had a sensitivity of 71.6, 71.4, and 72.0%, respectively, and a specificity of 55.5, 64.3, and 51.2%, respectively, to detect non-transmural infarction defined by ceMRI. Data-based and bootstrap-based sensitivities and specificities as well as the corresponding 95% CI for all myocardial deformation parameters are given in *Table 4*. Data-based and bootstrap-based sensitivities and specificities are almost identical for all deformation parameters.

Table 3 Sensitivity and specificity of myocardial deformation parameters for distinction between non-transmural infarction defined as hyperenhancement 1–50% and transmural myocardial infarction defined as >50% hyperenhancement by ceMRI

	Data-based estimate	Bootstrap-based estimate	95% Bootstrap CI	
			Lower limit	Upper limit
Circumferential strain				
Sensitivity (%)	70.4	69.3	64.4	74.5
Specificity (%)	71.2	69.7	65.3	74.7
Cut-off value (%)	≤−11.10	≤−10.70	−11.30	−10.40
Circumferential SR				
Sensitivity (%)	70.6	70.2	65.2	75.1
Specificity (%)	60.1	58.9	54.8	63.0
Cut-off value (s^{-1})	≤−1.00	≤−1.00	−1.03	−0.95
Radial strain				
Sensitivity (%)	70.0	66.8	61.7	72.0
Specificity (%)	71.2	68.4	63.8	72.9
Cut-off value (%)	>16.50	15.08	13.30	17.00
Radial SR				
Sensitivity (%)	70.1	69.2	64.3	74.1
Specificity (%)	70.6	69.7	65.0	74.0
Cut-off value (s^{-1})	>1.06	>1.05	1.01	1.10

Strain and SR related to myocardial wall thickness without hyperenhancement

Remaining myocardial wall thickness without hyperenhancement had a significant impact on circumferential (rmANCOVA, $P<0.001$) and radial strain (rmANCOVA, $P<0.001$) as well as on circumferential SR (rmANCOVA, $P<0.001$) and radial SR (rmANCOVA, $P<0.001$). The thicker the remaining myocardial wall thickness without hyperenhancement, the higher the myocardial deformation parameters (*Figure 5*).

Discussion

This study demonstrates that (i) myocardial deformation parameters obtained from frame-to-frame tracking of acoustic markers in 2D echocardiographic images allow distinction between different degrees of myocardial hyperenhancement defined by ceMRI; (ii) myocardial deformation parameters allow a reliable differentiation of transmural myocardial necrosis from non-transmural myocardial necrosis; (iii) the level of myocardial deformation relates to the wall thickness without hyperenhancement by ceMRI.

Table 4 Sensitivity and specificity of myocardial deformation parameters for distinction between non-infarction defined as hyperenhancement 0% and non-transmural myocardial infarction defined as 1–50% hyperenhancement by ceMRI

	Data-based estimate	Bootstrap-based estimate	95% Bootstrap CI	
			Lower limit	Upper limit
Circumferential strain				
Sensitivity (%)	71.4	70.4	62.2	78.3
Specificity (%)	64.3	63.9	60.1	67.7
Cut-off value (%)	>-16.50	>-16.68	-17.60	-15.70
Circumferential SR				
Sensitivity (%)	72.0	71.5	63.6	78.9
Specificity (%)	51.2	51.1	48.1	54.3
Cut-off value (s^{-1})	>-1.40	>-1.40	-1.44	-1.33
Radial strain				
Sensitivity (%)	70.1	69.5	60.7	78.7
Specificity (%)	57.2	56.9	53.4	60.4
Cut-off value (%)	≤ 27.10	≤ 27.40	25.50	29.40
Radial SR				
Sensitivity (%)	71.6	71.2	62.9	78.8
Specificity (%)	55.5	55.4	52.2	58.8
Cut-off value (s^{-1})	≤ 1.35	≤ 1.36	1.29	1.44

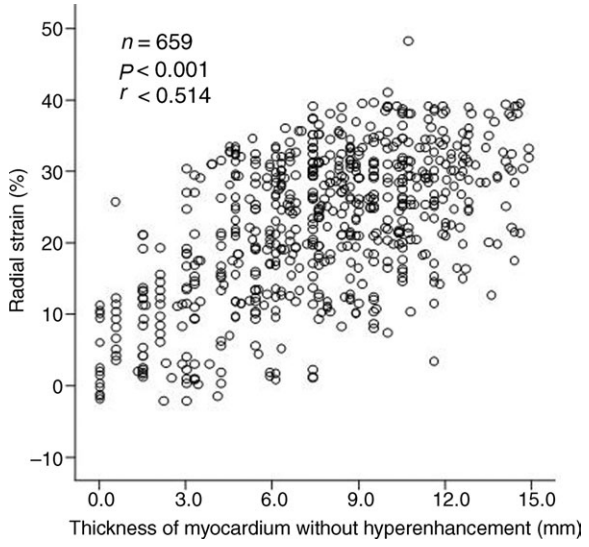

Figure 5 Correlation between wall thickness without late enhancement determined by cardiac magnetic resonance imaging and radial strain.

Assessment of myocardial viability

The accurate evaluation of myocardial viability in segments with impaired function has important clinical implications. Revascularization procedures are beneficial only in case of sufficient viable myocardium, whereas transmurally infarcted myocardium does not benefit.

Experimental echocardiographic studies using Doppler-derived myocardial deformation parameters have allowed differentiation of non-transmural infarcts from transmural infarcts.[10,11,21] Most Doppler-based deformation imaging techniques have been performed in the experimental setting, with analysis limited to myocardial segments perpendicular to the Doppler beam allowing undisturbed analysis of myocardial deformation between endocardium and epicardium. The clinical setting is characterized by more complex imaging conditions. In particular, there may be a considerable angle between Doppler beam and the connecting line between endocardium and epicardium in many cases. However, experimental studies have demonstrated Doppler-based myocardial strain and SR analysis to be significantly angle-dependent.[12] Furthermore, Doppler-based SR analysis is affected by significant noise artefacts. Thus, analysis of myocardial deformation between endocardium and epicardium on the basis of tissue Doppler imaging techniques, although very helpful in the experimental setting, has found only limited application in clinical practice.

Current study

The technique applied in this study on the basis of 2D echocardiography tracks acoustic markers from frame-to-frame. Compared with previous Doppler-based studies which determined strain and SR on the basis of velocity gradients between different points in space, definition of deformation parameters based on the tracking of acoustic markers relates to different distances in movement over time between different points in space. Because of the association of velocity and distance by the factor time, strain and SR defined on Doppler-based analysis or pixel-tracking-based analysis come to similar results, as has been shown previously.[22] However, the technique allows an angle-independent determination of strain and SR parameters.[23]

In the present study, an accurate differentiation between different degrees of transmurality in myocardial infarction could be obtained by the analysis of peak systolic strain and SR values. Furthermore, the level of myocardial deformation defined by the strain and SR parameters related also to the wall thickness without hyperenhancement. In particular, in chronic myocardial infarction with reduction of the total wall thickness, the thickness of the remaining myocardium without hyperenhancement may be a better parameter to define myocardial viability and the potential for functional recovery after revascularization than the relative amount of hyperenhancement.

The results of this study extend previous reports on this new imaging modality which have demonstrated that myocardial deformation parameters based on tissue pixel tracking allow differentiation of normal and clinically defined infarcted myocardium. In a study on 20 patients with myocardial infarction and 10 healthy volunteers, a significant difference in peak systolic strain and SR parameters could be shown between normal segments and infarct segments.[14]

Future studies will have to show whether myocardial deformation parameters allow also prediction of functional recovery after revascularization procedures with similar accuracy as well-established imaging techniques.

Limitations

As in all studies comparing different imaging modalities, there was the possibility of misalignment in segmental

data obtained by ceMRI and myocardial deformation imaging. Analysis of myocardial hyperenhancement by ceMRI sequence is prone to artefacts associated with the patient movements or inadequate breath-holding, which can be interpreted as areas of hyperenhancement by mistake. Quantitative analysis of the extent of hyperenhancement has been described.[24,25] However, visual analysis of hyperenhancement in ceMRI has been used in multiple previous studies and is considered very reliable due to the excellent image quality in most cases.[5] In this study, visual analysis of ceMRI was associated with a little inter- and intraobserver variability. Strain values were not zero in completely non-viable segments. This may be due to measurement artefacts related to tethering from adjacent segments. These artefacts are likely to have affected in particular segments with low myocardial deformation. However, in spite of these artefacts, a distinction of hyperenhancement categories was still possible.

The detection of non-transmural infarction vs. no infarction was associated with a low specificity for all parameters. However, in clinical practice, distinction of non-transmural vs. no infarction is of less importance than distinction of transmural vs. non-transmural infarction. Despite the good results in the bootstrap analysis, validation of results in an independent study is recommended.

Conclusion

This study demonstrates that myocardial deformation parameters obtained by tracking of acoustic markers within 2D echocardiographic images can be used to analyse transmurality of myocardial necrosis in patients with chronic depression of LV function due to myocardial infarction. The high applicability and reliable measurements obtained by this technique may make it a very helpful clinical tool to determine transmurality of myocardial necrosis.

Conflict of interest: none declared.

References

1. Wijns W, Vatner SF, Camici PG. Mechanisms of disease: hibernating myocardium. *N Engl J Med* 1998;**339**:173–181.
2. Pierard LA, De Landsheere CM, Berthe C, Rigo P, Kulbertus HE. Identification of viable myocardium by echocardiography during dobutamine infusion in patients with myocardial infarction after thrombolytic therapy: comparison with positron emission tomography. *J Am Coll Cardiol* 1990;**15**:1021–1031.
3. Dilsizian V, Rocco TP, Freddman NMT, Leon MB, Bonow RO. Enhanced detection of ischaemic but viable myocardium by the reinjection of thallium after stress-redistribution imaging. *N Engl J Med* 1990;**323**:141–146.
4. Tillisch J, Brunken R, Marshall R, Schwaiger M, Mandelkern M, Phelps M, Schelbert H. Reversibility of cardiac wall-motion abnormalities by positron tomography. *N Engl J Med* 1986;**314**:884–888.
5. Fieno DS, Kim RJ, Chen EL, Lomasney JW, Klocke FJ, Judd RM. Contrast-enhanced magnetic resonance imaging of myocardium at risk: distinction between reversible and irreversible injury throughout infarct healing. *J Am Coll Cardiol* 2000;**36**:1985–1991.
6. Kim RJ, Wu E, Rafael A, Chen EL, Parker MA, Simonetti O, Klocke FJ, Bonow RO, Judd RM. The use of contrast-enhanced magnetic resonance imaging to identify reversible myocardial dysfunction. *N Engl J Med* 2000;**343**:1445–1453.
7. Wagner A, Mahrholdt H, Holly TA, Elliott MD, Regenfus M, Parker M, Klocke FJ, Bonow RO, Kim RJ, Judd RM. Contrast-enhanced MRI and routine single photon emission computed tomography (SPECT) perfusion imaging for detection of subendocardial myocardial infarcts: an imaging study. *Lancet* 2003;**361**:374–379.
8. Heimdal A, Stoylen A, Torp H, Skjaerpe T. Real-time strain rate imaging of the left ventricle by ultrasound. *J Am Soc Echocardiogr* 1998;**11**:1013–1019.
9. D'hooge J, Bijnens B, Thoen J, Van de Werf F, Sutherland GR, Suetens P. Echocardiographic strain and strain-rate imaging: a new tool to study regional myocardial function. *IEEE Trans Med Imaging* 2002;**21**:1022–1030.
10. Derumeaux G, Loufoua J, Pontier G, Cribier A, Ovize M. Tissue Doppler imaging differentiates transmural from nontransmural acute myocardial infarction after reperfusion therapy. *Circulation* 2001;**103**:589–596.
11. Weidemann F, Dommke C, Bijnens B, Claus P, D'hooge J, Mertens P, Verbeken E, Maes A, Van de Werf F, De Scheerder I, Sutherland GR. Defining the transmurality of a chronic myocardial infarction by ultrasonic strain-rate imaging. *Circulation* 2003;**107**:883–888.
12. Urheim S, Edvardsen T, Torp H, Angelsen B, Smiseth OA. Myocardial strain by Doppler echocardiography: validation of a new method to quantify regional myocardial function. *Circulation* 2000;**102**:1158–1164.
13. Reisner S, Lysyansky P, Agmon Y, Mutlak D, Lessick J, Friedman Z. Global longitudinal strain: a novel index of left ventricular systolic function. *J Am Soc Echocardiogr* 2004;**17**:630–633.
14. Leitman M, Lysyansky P, Sidenko S, Shir V, Peleg E, Binenbaum M, Kaluski E, Krakover R, Vered Z. Two-dimensional strain—a novel software for real-time quantitative echocardiographic assessment of myocardial function. *J Am Soc Echocardiogr* 2004;**17**:1021–1029.
15. Schiller NB, Shah PM, Crawford M, DeMaria A, Devereux R, Feigenbaum H, Gutgesell H, Reichek N, Sahn D, Schnittger I. Recommendations for quantitation of the left ventricle by two-dimensional echocardiography. American Society of Echocardiography Committee on Standards, Subcommittee on Quantitation of Two-Dimensional Echocardiograms. *J Am Soc Echocardiogr* 1989;**2**:358–367.
16. Lin LIK. A concordance correlation coefficient to evaluate reproducibility. *Biometrics* 1989;**45**:255–268.
17. Kim RJ, Wu E, Rafael A, Chen EL, Parker MA, Simonetti O, Klocke FJ, Bonow RO, Judd RM. The use of contrast-enhanced magnetic resonance imaging to identify reversible myocardial dysfunction. *N Engl J Med* 2000;**343**:1445–1453.
18. Kim RJ, Fieno DS, Parrish TB, Harris K, Chen EL, Simonetti O, Bundy J, Finn JP, Klocke FJ, Judd RM. Relationship of MRI delayed contrast enhancement to irreversible injury, infarct age and contractile function. *Circulation* 1999;**100**:1992–2002.
19. Cohen J. A coefficient of agreement for nominal scales. *Educ Psychol Meas* 1960;**20**:37–46.
20. Efron B, Tibshirani RJ. *An Introduction to the Bootstrap*. New York: Chapman and Hall; 1993.
21. Zhang Y, Chan AKY, Yu CM, Yip GWK, Fung JWH, Lam WWM, So NMC, Wang M, Wu EB, Wong JT, Sanderson JE. Strain rate imaging differentiates transmural from non-transmural myocardial infarction. *J Am Coll Cardiol* 2005;**46**:864–871.
22. Hanekom L, Jeffries L, Haluska B, Marwick TH. 2D strain—new approach to strain and strain rate: the solution to the angle-dependence of tissue Doppler? (Abstract). *Eur Heart J* 2004;**25**:P2862.
23. Langeland S, D'hooge J, Wouters PF, Leather A, Claus P, Bijnens B, Sutherland GR. Experimental validation of a new ultrasound method for the simultaneous assessment of radial and longitudinal myocardial deformation independent of insonation angle. *Circulation* 2005;**112**:2157–2162.
24. Kühl HP, Beek AM, Van der Weerdt AP, Hofman MB, Visser CA, Lammertsma AA, Heussen N, Visser FC, van Rossum AC. Myocardial viability in chronic ischaemic heart disease. Comparison of contrast-enhanced magnetic resonance imaging with 18F-fluorodeoxyglucose positron emission tomography. *J Am Coll Cardiol* 2003;**41**:1341–1348.
25. Klein C, Nekolla SG, Bengel FM, Momose M, Sammer A, Haas F, Schnackenburg B, Delius W, Mudra H, Wolfram D, Schwaiger M. Assessment of myocardial viability with contrast-enhanced magnetic resonance imaging: comparison with positron emission tomography. *Circulation* 2002;**105**:162–167.